

Thermophysics of alkali and related azides

I. Heat capacity of NaN, from 5 to 350 K ^a

ROBERT W. CARLING^b and EDGAR F. WESTRUM, JR.^c

*Department of Chemistry, University of Michigan, Ann Arbor,
Michigan 48104, U.S.A.*

(Received 6 January 1976)

The heat capacity of sodium azide was determined from 5 to 350 K by adiabatic calorimetry and a thermal anomaly associated with a structural transformation of the crystalline lattice was observed in the heat capacity at (293.0 ± 0.1) K. The excess entropy associated with this transition was determined to be only (0.008 ± 0.001) cal_{th} K⁻¹ mol⁻¹. At 298.15 K, the values for C_p , S , $\{H(T) - H(0)\}/T$, and $-\{G(T) - H(0)\}/T$, respectively, are 18.31, 23.15, 11.813, and 11.340 cal_{th} K⁻¹ mol⁻¹.

Introduction

Since the preparation of the first azide, phenyl azide, by Griess in 1866,⁽¹⁾ both organic and inorganic azides have always been thought remarkable, especially for the symmetry of the azide ion and the wide range of stability of the compounds. The symmetrical linear azide ion, N₃⁻, occurs in ionic salts such as the alkali-metal azides; asymmetrical azide groups appear in covalently-bonded environments of organic azides.

All of the alkali-metal hydrogen difluorides are isostructural with the corresponding alkali-metal azides. At 300 K the sodium salts are rhombohedral and the potassium, rubidium, and cesium salts are tetragonal. The linear symmetrical anions of both the hydrogen difluorides and the azides possess 16 valence electrons. These structural similarities suggest that the thermal behavior of the corresponding hydrogen difluorides and azides should also be similar. The crystal structure of sodium azide is a distorted rhombohedral NaCl-type structure with space group R_{3m}-D_{3d}⁵.⁽²⁾ The distortion may be visualized by substituting an azide ion for a chloride ion in NaCl thus compressing the structure in one direction and extending it in the other. The structure of NaN₃ is that of a sandwich made up of alternating layers of sodium and azide ions; each species of ion is surrounded by six of the other species.

Sodium azide is known to undergo a phase transition at 292 K⁽³⁾ in contrast to the behavior observed in NaHF₂,⁽⁴⁾ where an anomaly observed in the heat capacity

^a This work has been supported in part by the National Science Foundation, Chemical Thermodynamics Contract GP-42525X.

^b Abstracted in part from a dissertation submitted to the Horace H. Rackham School of Graduate Studies at the University of Michigan in partial fulfillment of the requirements for the Ph.D. degree.

^c To whom correspondence concerning this paper should be directed.

of NaHF_2 was ascertained to be due to contamination of the calorimetric sample by a slight excess of hydrogen fluoride.

Low-temperature adiabatic calorimetry permitted determination of the heat capacity of sodium azide and delineation of the energetics of the lattice transformation.

Experimental

SAMPLE PREPARATION AND CHARACTERIZATION

Sodium azide (anhydrous) purchased from Matheson, Coleman, and Bell was reported to have a purity in excess of 98 mass per cent. The sample was first dissolved in water and then filtered to remove any insoluble impurities. The filtrate was then evaporated by heating until incipient crystallization occurred and then allowed slowly to cool to 300 K. The calorimetric sample was recrystallized from water three times. The thin tabular crystals that formed upon cooling were filtered, washed with pure ethanol, and then dried for several hours in an oven at 380 K and stored in a desiccator over calcium sulfate.

X-Ray diffraction analysis of hexagonally indexed sodium azide yielded lattice parameters which agree well with those of other investigators (see table 1). A complete

TABLE 1. Derived lattice parameters of NaN_3

Reference	8	9	10	4	this work ^a
<i>a</i> /nm	0.362	0.363	0.3646	0.3638	0.3647 ± 0.0002
<i>c</i> /nm	1.510	1.519	1.5213	1.5201	1.522 ± 0.003

^a Guinier, $\text{CuK}\alpha_1$. Calculated from a least-squares fit of 7 indexed lines. The uncertainties represent three standard deviations.

tabulation, of the measured *d*-spacings for this sample has been reported previously⁽⁵⁾ and is also available as a supplementary document.⁽⁶⁾

The sodium content of sodium azide was determined gravimetrically,⁽⁷⁾ by conversion to sodium sulfate subsequently fired to constant mass in a Lindberg furnace at 1140 K. Similarly treated sodium chloride served as a standard in the determination of sodium. The elemental analysis indicated (35.45 ± 0.03) mass per cent of sodium (theoretical: 35.36).

CALORIMETRIC PROCEDURES

Heat-capacity measurements on sodium azide were made in the Mark II cryostat previously described.⁽¹¹⁾ The calorimeter (laboratory designation W-28, about 92 cm³ volume) used was a gold-plated thin-walled copper container with radial vanes to enhance thermal equilibration of the sample and container. The calorimetric sample of sodium azide had a mass of 41.0627 g and the heat capacity of the sample always exceeded 64 per cent of the total. Buoyancy corrections were based on a density for NaN_3 of 1.84 g cm⁻³. Helium at a pressure of 44 Torr† at 300 K was

† Throughout this paper Torr = (101.325/760) kPa, $\text{cal}_{\text{th}} = 4.184 \text{ J}$.

used to facilitate achievement of rapid equilibrium in the calorimeter. All measurements of mass, temperature, resistance, potential, and time are referred to standardizations and calibrations performed at the National Bureau of Standards.

Results and discussion

THERMODYNAMIC PROPERTIES

The experimental heat capacities for sodium azide are presented in chronological sequence at the mean temperatures of determination in table 2 and are displayed in figure 1. Temperature increments employed in the measurements may usually be

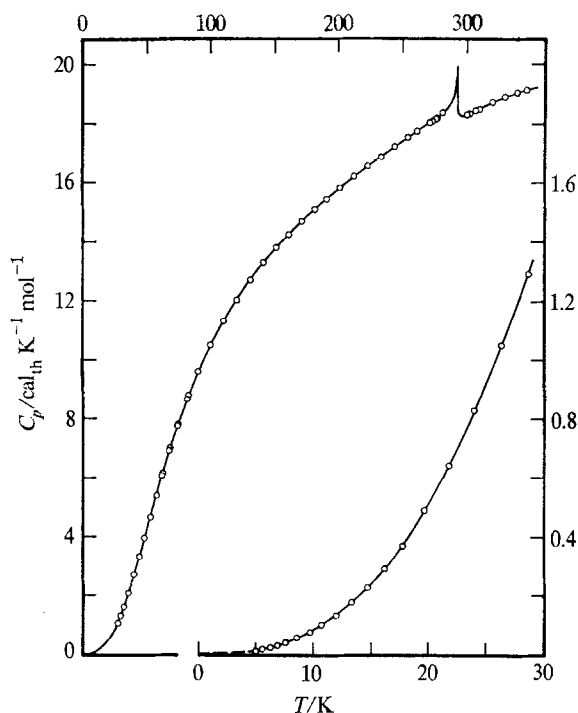


FIGURE 1. Heat capacity of sodium azide.

inferred from the differences in the adjacent mean temperatures. These results have been adjusted for curvature and are considered to have a probable error of about 5 per cent at 5 K, decreasing to 1.0 per cent at 10 K, and to less than 0.1 per cent above 20 K. The values are based upon the IPTS-48, and a molar mass of $65.010 \text{ g mol}^{-1}$ for NaN_3 . Results from several series of determinations taken to ascertain the enthalpy increment through the transition region have been summarized in table 3. The smoothed heat capacities and associated thermodynamic functions presented in table 4 were obtained by processing the experimental results using a high-speed digital computer. The thermodynamic functions have a probable error of less than

TABLE 2. Heat capacity of NaN_3
 ($\text{cal}_{\text{th}} = 4.184 \text{ J}$)

$\frac{T}{\text{K}}$	$\frac{C_p}{\text{cal}_{\text{th}} \text{K}^{-1} \text{mol}^{-1}}$	$\frac{T}{\text{K}}$	$\frac{C_p}{\text{cal}_{\text{th}} \text{K}^{-1} \text{mol}^{-1}}$	$\frac{T}{\text{K}}$	$\frac{C_p}{\text{cal}_{\text{th}} \text{K}^{-1} \text{mol}^{-1}}$	$\frac{T}{\text{K}}$	$\frac{C_p}{\text{cal}_{\text{th}} \text{K}^{-1} \text{mol}^{-1}}$
	Series I		Series II	74.10	7.789	24.08	0.826
73.97	7.770	261.44	17.84	82.45	8.810	26.43	1.050
81.22	8.661	271.53	18.07			28.72	1.291
90.00	9.619	281.68	18.40		Series VI	31.31	1.592
99.96	10.52	291.71	18.70		(see below)	34.85	2.053
109.93	11.32	301.73	18.35			39.20	2.670
120.21	12.05				Series VII	43.50	3.310
130.96	12.73		Series III	5.02	0.012	47.65	3.946
141.22	13.31		(see below)	5.60	0.016	52.13	4.650
151.10	13.81			6.30	0.023	56.87	5.377
161.11	14.27		Series IV	6.93	0.029	62.06	6.165
171.29	14.71	275.85	18.20	7.63	0.039	68.09	7.010
181.22	15.11		ΔH Detn. A	8.56	0.056		
190.95	15.46	309.96	18.50	9.64	0.080		Series VIII
201.32	15.85	319.92	18.73	10.78	0.105	274.91	18.18
212.32	16.22	329.80	18.90	12.02	0.131		ΔH Detn. B
223.13	16.58	339.62	19.06	13.36	0.173	307.69	18.47
233.77	16.91	346.98	19.12	14.73	0.226		
244.24	17.26			16.24	0.290		Series IX
254.55	17.60		Series V	17.84	0.368		(see below)
		61.51	6.084	19.70	0.486		
		67.30	6.909	21.84	0.641		

$\frac{T}{\text{K}}$	$\frac{\Delta T}{\text{K}}$	$\langle C_p \rangle$ ^a $\frac{\text{cal}_{\text{th}} \text{K}^{-1} \text{mol}^{-1}}$	C_p ^b $\frac{\text{cal}_{\text{th}} \text{K}^{-1} \text{mol}^{-1}}$	$\frac{T}{\text{K}}$	$\frac{\Delta T}{\text{K}}$	$\langle C_p \rangle$ ^a $\frac{\text{cal}_{\text{th}} \text{K}^{-1} \text{mol}^{-1}}$	C_p ^b $\frac{\text{cal}_{\text{th}} \text{K}^{-1} \text{mol}^{-1}}$
		Series III		292.24	0.22	19.36	19.29
273.62	10.28	18.13	18.13	292.45	0.22	19.48	19.39
281.80	6.10	18.39	18.40	292.66	0.22	19.49	19.51
285.85	2.02	18.66	18.54	292.87	0.22	19.57	19.69
287.86	2.01	18.66	18.65	293.08	0.22	19.52	19.52
289.86	2.00	18.82	18.82	293.30	0.22	18.92	18.92
291.84	1.98	19.11	19.16	293.62	0.45	18.37	18.37
293.83	2.02	18.54	18.39	294.07	0.45	18.31	18.31
295.86	2.05	18.18	18.24				
297.89	2.04	18.26	18.26			Series IX	
300.93	4.07	18.33	18.33	288.65	3.54	18.75	18.71
				290.63	0.43	18.90	18.92
		Series VI		291.04	0.43	18.98	18.98
286.86	1.91	18.59	18.50	291.46	0.42	19.04	19.06
288.75	1.90	18.74	18.71	291.88	0.42	19.07	19.16
289.84	0.32	18.79	18.82	292.19	0.21	19.33	19.25
290.21	0.44	18.82	18.86	292.39	0.21	19.36	19.36
290.64	0.44	18.94	18.92	292.59	0.21	19.42	19.46
291.08	0.44	19.12	18.98	292.80	0.21	19.61	19.61
291.40	0.22	19.05	19.05	293.00	0.21	19.95	19.95
291.61	0.22	19.10	19.10	293.31	0.43	18.92	18.46
291.82	0.22	19.13	19.15	293.73	0.44	18.34	18.35
292.03	0.22	19.20	19.21				

^a The symbol $\langle C_p \rangle$ represents mean values of the heat capacity as calculated directly from finite $\Delta H/\Delta T$ without curvature correction.

^b The symbol C_p in columns adjacent to $\langle C_p \rangle$ represents the value of the heat capacity read from the smoothed curve at temperature T . Elsewhere in the table it represents C_p analytically corrected for curvature.

TABLE 3. Enthalpy determinations for sodium azide
($\text{cal}_{\text{th}} = 4.184 \text{ J}$)

Designation	T_1 K	T_2 K	$\frac{\{H(T_2) - H^\circ(T_1)\}}{\text{cal}_{\text{th}} \text{ mol}^{-1}}$	$\frac{\{H^\circ(305 \text{ K}) - H^\circ(275 \text{ K})\}}{\text{cal}_{\text{th}} \text{ mol}^{-1}}$
A (Series IV)	280.92	304.97	445.98	554.79
B (Series VIII)	279.78	302.89	428.79	554.95
Series II	276.63	306.78	558.37	554.21
				Mean: 554.6 ± 0.5

0.1 per cent above 50 K. Below 5 K the heat capacities were extrapolated using the Debye T^3 limiting law. The entropies and Gibbs functions have not been adjusted for nuclear spin and isotopic mixing contributions, and hence are practical values for use in chemical thermodynamic calculations.

TRANSITION

A detailed picture of the transition observed in sodium azide at $(293.0 \pm 0.1) \text{ K}$ is shown in figure 2. The values of the enthalpy and entropy of transition were derived as follows. The estimated lattice heat capacity was extrapolated as indicated by the

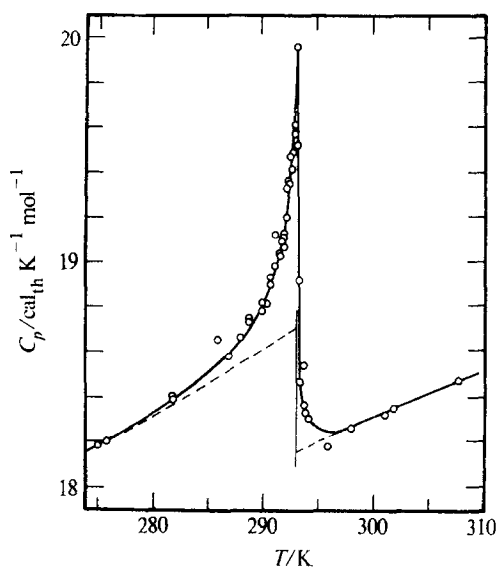


FIGURE 2. Heat capacity of sodium azide in the transition region.

dashed line in figure 2, to the temperature of the heat-capacity maximum. To determine the lattice heat capacity over the transition region, a large-scale plot of effective Θ_D against temperature was made and the trend in the lattice curvature of Θ_D against T was extrapolated to 293 K from below and above the transition. From these estimated Θ_D 's and their respective temperatures the lattice heat capacities between

TABLE 4. Standard molar thermodynamic functions of sodium azide NaN_3
 ($\text{cal}_{\text{th}} = 4.184 \text{ J}$)

T K	C_p $\text{cal}_{\text{th}} \text{K}^{-1} \text{mol}^{-1}$	$\{S^\circ(T) - S^\circ(0)\}$ $\text{cal}_{\text{th}} \text{K}^{-1} \text{mol}^{-1}$	$\{H^\circ(T) - H^\circ(0)\}$ $\text{cal}_{\text{th}} \text{mol}^{-1}$	$-\{G^\circ(T) - H^\circ(0)\}/T$ $\text{cal}_{\text{th}} \text{K}^{-1} \text{mol}^{-1}$
5	0.010	(0.004)	(0.014)	(0.001)
10	0.083	0.030	0.223	0.008
15	0.236	0.089	0.980	0.024
20	0.505	0.191	2.780	0.052
25	0.908	0.345	6.258	0.094
30	1.439	0.555	12.075	0.153
35	2.075	0.824	20.822	0.229
40	2.784	1.146	32.945	0.323
45	3.539	1.517	48.739	0.434
50	4.324	1.931	68.39	0.563
60	5.851	2.855	119.33	0.867
70	7.263	3.865	185.02	1.222
80	8.517	4.919	264.06	1.618
90	9.605	5.986	354.80	2.044
100	10.541	7.048	455.64	2.491
110	11.347	8.091	565.2	2.953
120	12.049	9.109	682.2	3.424
130	12.670	10.099	805.9	3.900
140	13.229	11.059	935.4	4.377
150	13.739	11.989	1070.3	4.853
160	14.211	12.891	1210.1	5.328
170	14.650	13.766	1354.4	5.799
180	15.06	14.615	1503.0	6.265
190	15.45	15.44	1655.6	6.726
200	15.82	16.24	1811.9	7.182
210	16.16	17.02	1971.8	7.632
220	16.49	17.78	2135.1	8.076
230	16.80	18.52	2301.6	8.514
240	17.11	19.24	2471.2	8.946
250	17.41	19.95	2643.8	9.372
260	17.72	20.64	2819.4	9.792
270	18.05	21.31	2998.2	10.207
280	18.45	21.97	3180.6	10.615
290	18.97	22.63	3367.6	11.018
293.0 ^a	19.95			
300	18.33	23.27	3555.9	11.414
310	18.50	23.87	3740.0	11.806
320	18.70	24.46	3926.0	12.192
330	18.91	25.04	4114.0	12.573
340	19.09	25.61	4304.0	12.948
350	19.21	26.16	4495.6	13.317
273.15	18.17	21.52	3055.2	10.336
298.15	18.31	23.15	3522.0	11.340

^a Peak of transition.

275 and 305 K were calculated. The dashed line in figure 2 represents the C_p values obtained in this fashion. The experimental heat capacity curve and the estimated lattice were then separately integrated (see table 3). To determine the enthalpy and entropy of transition, the difference between the two curves was taken. The lattice enthalpy $\{H(305 \text{ K}) - H(275 \text{ K})\}$ was determined to be $551.7 \text{ cal}_{\text{th}} \text{ mol}^{-1}$. The resulting entropy and enthalpy of transition were found to be $\Delta S_t = (0.008 \pm 0.001) \text{ cal}_{\text{th}} \text{ K}^{-1} \text{ mol}^{-1}$ and $\Delta H_t = (2.91 \pm 0.55) \text{ cal}_{\text{th}} \text{ mol}^{-1}$.

Different cooling rates through the transition had no effect on the overall enthalpy between 275 and 305 K. On a cooling curve through the transition region recorded as a function of time, the intersection of the slopes of the cooling lines taken above and below the transition was at about 293 K. This indicated that the transition was easily reversible and free of significant hysteresis.

The phase transition observed in this research was first detected by differential thermal analysis in 1957,⁽¹²⁾ however, that work remains unpublished. Subsequent to the discovery of the phase transition in sodium azide, Bradley *et al.*⁽¹³⁾ were able to demonstrate the existence of the transition on the phase diagram at high pressures. High-pressure X-ray diffraction on crystalline powders showed a splitting of the diffraction lines (indicative of the transition) at approximately 250 MPa pressure.

Miller and King⁽³⁾ observed a transition in sodium azide crystals doped with a mass fraction 5×10^{-6} of Mn^{+2} at $(292 \pm 1) \text{ K}$ by electron spin resonance (e.s.r. spectral scans) as a function of temperature. The change in crystal field as seen in the e.s.r. spectrum indicated a structural change in the host crystal. Their powder results were taken to indicate a reduction in symmetry from hexagonal to orthorhombic crystal structure upon reduction of temperature; however, their indexing of the low-temperature phase as orthorhombic was later demonstrated to be incorrect⁽¹⁰⁾ because too few powder lines were observed.

Satoh and Sogabe⁽¹⁴⁾ measured the mean specific heat capacity of sodium azide from 273 to 373 K with an ice calorimeter to ascertain the heat capacity contribution of nitrogen rather than to examine the transition. The heat capacity of sodium azide was measured by Fritzer and Torkar⁽¹⁵⁾ from 250 to 575 K by continuous-heating adiabatic calorimetry. The reproducibility of their results was estimated to be about 0.3 per cent between 250 and 380 K, about 0.5 per cent between 380 and 470 K, and 0.8 per cent above 470 K. At temperatures between 100 and 350 K our present results have a reproducibility of 0.1 per cent. The authors did observe heat capacities higher than their precision indices in the vicinity of 293 K and attributed this to the transition reported by Miller and King.⁽³⁾ Their method of obtaining results was not conducive to the accurate study of enthalpies of phase changes and, therefore, they did not directly measure the energy of the solid-to-solid transformation. They estimated ΔH_t to be between 10 to $20 \text{ cal}_{\text{th}} \text{ mol}^{-1}$.

Using both single crystals and powder samples, Pringle and Noakes,⁽¹⁰⁾ showed that the low-temperature form of NaN_3 was monoclinic with space group $C2/m$. They proposed that the low-temperature phase be labelled α and the high-temperature form β . They found that the anion units differ in their orientation along the hexagonal c -axis in phase α and in phase β and that one of the terminal nitrogen atoms comes

closer to one sodium than to the other two. Hence, this distortion in transforming from the α - to the β -form upon reducing the temperature may be described mainly as one of shear of the Na atoms incorporating a contraction of the lattice along the monoclinic a -axis. The unit-cell volume (per molecule) decreases by about 2 per cent between 300 and 173 K.

Following the arguments presented by Pringle and Noakes,⁽¹⁰⁾ Iqbal^(16, 17) demonstrated from Raman scattering experiments that the phase change in sodium azide may be of second-order character. The order-disorder mechanism in sodium azide is related to the disappearance of the barrier to angular reorientation of the azide ions with respect to the c -axis. The change in frequency of the Raman active librational mode as a function of temperature was shown to be indicative of a second-order phase transition.⁽¹⁶⁾

Later work by Simonis and Hathaway⁽¹⁸⁾ involved a Raman-spectral study of the phase transition in sodium azide. Their results did not conform with either the standard displacive or order-disorder types of second-order transitions; but were not conclusive due to the undetermined behavior of NaN_3 near the transition point.

Our present heat-capacity studies on sodium azide seem to indicate the phase transition to be of second order. This conclusion is based on a finite heat capacity of about $20 \text{ cal}_{\text{th}} \text{ K}^{-1} \text{ mol}^{-1}$ at the peak of transition, together with the negligible change in volume (less than 0.1 per cent⁽¹⁸⁾) between α - and β - NaN_3 .

Lithium azide does not show the same type of structural behavior as sodium azide. Lithium azide was found to be isostructural with α - NaN_3 .⁽¹⁰⁾ Since no polymorphic transformation was observed up to 1 GPa in LiN_3 ,⁽¹³⁾ the transformation in LiN_3 lies either at higher pressures or at temperatures above its decomposition temperature. Iqbal⁽¹⁶⁾ has postulated, by analogy with NaN_3 , a phase transition occurring at 262 K for lithium azide. If this is true, the LiN_3 phase below 262 K certainly is not isostructural with α - or β - NaN_3 . If a low-temperature phase LiN_3 does appear at atmospheric pressure it may well be isostructural with a high-pressure sodium azide phase of unknown structure observed by Pistorius and White⁽¹⁹⁾ and designated NaN_3 -III. Heat-capacity measurements on LiHF_2 over the temperature range 5 to 300 K⁽⁴⁾ do not indicate any structural modifications.

Although the similarities between the thermophysical properties of potassium, rubidium, and cesium azides and the corresponding hydrogen difluorides are striking,^(5, 6) these similarities seem not to extend to the sodium salts. One might postulate that the structural transition in NaHF_2 was obscured by the anomaly stemming from non-stoichiometry of the NaHF_2 sample. However, it was found possible to cool NaHF_2 only several kelvins below its thermal anomaly and measure heat capacities in the anomalous region which agreed with values interpolated from values adjacent to this region; these observations seem to exclude the occurrence of a structural change in NaHF_2 in this temperature region. Hence, although the entropy at 298.15 K for NaHF_2 is $21.73 \text{ cal}_{\text{th}} \text{ K}^{-1} \text{ mol}^{-1}$,⁽⁴⁾ in comparison with the corresponding entropy for NaN_3 ($23.15 \text{ cal}_{\text{th}} \text{ K}^{-1} \text{ mol}^{-1}$), a discrepancy of about 7 per cent (which approximates $R \ln 2$), the X-ray diffraction data⁽²⁰⁾ on NaHF_2 do not suggest a basis for ascribing residual entropy to NaHF_2 .

REFERENCES

1. Griess, P. *Ann. Chim. Phys.* **1866**, 137, 39.
2. Hendricks, S. B.; Pauling, L. *J. Amer. Chem. Soc.* **1925**, 47, 2904.
3. Miller, B. S.; King, G. J. *J. Chem. Phys.* **1963**, 39, 2779.
4. Westrum, E. F., Jr.; Burney, G. A. *J. Phys. Chem.* **1961**, 65, 344.
5. Carling, R. W., Ph.D. thesis, the University of Michigan, Ann Arbor, Michigan, **1975**.
6. For detailed supplementary data concerning X-ray analysis of the sample used in this research, see NAPS document No. 02771 for 12 pages of supplementary material. Order from ASIS/NAPS, c/o Microfiche Publications, 305 E. 46th St., New York, N.Y. 10017. Remit in advance for each NAPS accession number. Make checks payable to Microfiche Publications. Photographs are \$5.00. Microfiche are \$3.00. Outside the U.S. or Canada postage is \$2.00 for a photocopy or \$1.00 for a fiche.
7. Vogel, A. I. *A Text-Book of Inorganic Analysis*, 3rd ed., John Wiley and Sons, Inc.: New York, **1961**.
8. West, C. D. *Z. Krist.* **1934**, 88, 97.
9. Catalog of X-Ray Powder Data, American Society for Testing and Materials, No. 1-0931.
10. Pringle, G. E.; Noakes, D. E. *Acta Crystallogr. Sect. B.* **1968**, 24, 262.
11. Westrum, E. F., Jr.; Furukawa, G. T.; McCullough, J. P. "Adiabatic Low-Temperature Calorimetry", In *Experimental Thermodynamics*, Vol. 1, McCullough, J. P.; Scott, D. W.; editors. Butterworths: London, **1968**.
12. Petz, J. University of Arkansas, **1957**, unpublished.
13. Bradley, R. S.; Grace, J. D.; Munro, D. C. *Z. Krist.* **1964**, 120, 349.
14. Sato, S.; Sogabe, T. *Bull. Inst. Phys. Chem. Res.* **1940**, 19, 943; *Sci. Papers Inst. Phys. Chem. Res.* **1941**, 38, 174.
15. Fritzer, H. P.; Torkar, K. *Monatsh. Chem.* **1966**, 97, 703.
16. Iqbal, Z. *J. Chem. Phys.* **1973**, 59, 1769.
17. Iqbal, Z. *Advan. Raman Spec.* **1972**, 1, 188.
18. Simonis, G. J.; Hathaway, C. E. *Phys. Rev. B* **1974**, 10, 4419.
19. Pistorius, C. W. F. T.; White, A. J. C. *High Temp.—High Pres.* **1970**, 2, 507.
20. Wyckoff, R. W. G. *Crystal Structures*, Vol. 2. Interscience: New York, **1964**, p. 277.